THE COMPANY OF Biologists

RESEARCH ARTICLE

Unsteady flow affects swimming energetics in a labriform fish (*Cymatogaster aggregata*)

D. G. Roche[1],*, M. K. Taylor[2], S. A. Binning[1], J. L. Johansen[3], P. Domenici[4] and J. F. Steffensen[5]

ABSTRACT

Unsteady water flows are common in nature, yet the swimming performance of fishes is typically evaluated at constant, steady speeds in the laboratory. We examined how cyclic changes in water flow velocity affect the swimming performance and energetics of a labriform swimmer, the shiner surfperch, *Cymatogaster aggregata*, during station holding. Using intermittent-flow respirometry, we measured critical swimming speed (U_{crit}), oxygen consumption rates ($\dot{M}_{O_2}$) and pectoral fin use in steady flow versus unsteady flows with either low- [0.5 body lengths (BL) s^{-1}] or high-amplitude (1.0 BL s^{-1}) velocity fluctuations, with a 5 s period. Individuals in low-amplitude unsteady flow performed as well as fish in steady flow. However, swimming costs in high-amplitude unsteady flow were on average 25.3% higher than in steady flow and 14.2% higher than estimated values obtained from simulations based on the non-linear relationship between swimming speed and oxygen consumption rate in steady flow. Time-averaged pectoral fin use (fin-beat frequency measured over 300 s) was similar among treatments. However, measures of instantaneous fin use (fin-beat period) and body movement in high-amplitude unsteady flow indicate that individuals with greater variation in the duration of their fin beats were better at holding station and consumed less oxygen than fish with low variation in fin-beat period. These results suggest that the costs of swimming in unsteady flows are context dependent in labriform swimmers, and may be influenced by individual differences in the ability of fishes to adjust their fin beats to the flow environment.

KEY WORDS: Complex flow, Critical swimming speed, Fin-beat frequency, Pectoral fin swimming, Oxygen consumption rate, Respirometry

INTRODUCTION

The energetic costs of locomotion comprise a large and variable component of the energy budgets of mobile organisms (Boisclair and Sirois, 1993). Environmental factors that influence locomotor costs can therefore have profound effects on individual fitness (Arnold, 1983; Irschick and Garland, 2001). In fishes, the energetic costs of swimming have traditionally been estimated by measuring oxygen consumption rates in steady (i.e. constant speed) water flows (e.g. Steffensen et al., 1984; Claireaux et al., 1995; Farrell et al., 2003;

[1]Australian Research Council Centre of Excellence for Coral Reef Studies, Research School of Biology, Australian National University, 116 Daley Road, Canberra, ACT 0200, Australia. [2]Department of Biology, Carleton University, 1125 Colonel By Drive, Ottawa, ON K1S 5B6, Canada. [3]Australian Research Council Centre of Excellence for Coral Reef Studies, School of Marine and Tropical Biology, James Cook University, Townsville, QLD 4811, Australia. [4]CNR – IAMC, Istituto per l'Ambiente Marino Costiero, Località Sa Mardini, 09072 Torregrande, Oristano, Italy. [5]University of Copenhagen, Marine Biological Laboratory, Biological Institute, Strandpromenaden 5, DK-3000 Helsingør, Denmark.

*Author for correspondence (dominique.roche@mail.mcgill.ca)

Clark et al., 2011). However, these measures may not reflect the true costs of swimming in nature, where the velocity of water flows can vary dramatically over short time scales (Liao, 2007; Webb et al., 2010). Increasingly, fish biologists and eco-physiologists are aware of the need to measure swimming costs in settings that approximate wild conditions both to improve our understanding of fish locomotion and for practical applications such as water and habitat management (Enders et al., 2003; Liao, 2007; Lacey et al., 2012).

In nature, water flow can be influenced by numerous physical variables including wind, gravity and obstructions below the surface, creating complex water flows (Liao, 2007; Webb et al., 2010). Terms used to describe flow hydrodynamics with regard to swimming are often not clearly defined, which makes generalizations about the effects of these complex flows on fishes difficult (see Liao 2007). Turbulence usually refers to the creation of vortices of variable strengths and sizes in flowing water, whereas unsteady flows can be near-laminar and are characterized by changes in fluid velocity over time at a given point in space (Liao 2007; Webb et al., 2010). Depending on the causal agent, turbulent flows may have an element of predictability that can be exploited by swimming fish (Liao et al., 2003a; Liao et al., 2003b; Liao, 2004; Beal et al., 2006; Cook and Coughlin, 2010; Taguchi and Liao, 2011). However, water flows with unpredictable and/or wide fluctuations in velocity are known to increase the costs of locomotion (Pavlov et al., 2000; Enders et al., 2003; Enders et al., 2005; Lupandin, 2005; Webb and Cotel, 2010). Whether unsteady flows represent advantages or disadvantages to swimming fishes remains an important area of research.

One major impediment to studying the effects of complex flows on fish locomotion is the challenge of creating describable and/or repeatable hydrodynamic perturbations in an experimental setting (Liao, 2007; Lacey et al., 2012). As a result, only a handful of studies have directly examined the metabolic costs of swimming in complex flows (Enders et al., 2003; Liao et al., 2003a; Cook and Coughlin, 2010; Tritico and Cotel, 2010; Taguchi and Liao, 2011). While extremely useful, these studies are restricted to fishes such as trout, salmon and minnows that use their body and caudal fin for propulsion (BCF swimmers). However, roughly 15–20% of all living fishes, including a large proportion of fishes in shallow marine (e.g. labrids, pomacentrids) and freshwater (e.g. cichlids, centrarchids) habitats, use their pectoral (i.e. paired) fins for swimming (MPF or labriform swimmers) (Westneat, 1996; Bellwood and Wainwright, 2001). Labriform swimmers are commonly found in habitats associated with complex flows (Fulton, 2010), especially inshore coastal habitats where wave-driven water motion varies considerably across local and regional gradients (Webb et al., 2010). For example, on the west coast of the United States, bays and sounds that are sheltered from large storm waves regularly experience wave-driven water flows ranging from 0 to 50 cm s^{-1} (Finlayson, 2006; Gaylord et al., 2008). Similarly, shallow coral reef habitats in the tropics are

The Journal of Experimental Biology

List of symbols

U_a	amplitude of flow velocity fluctuations (BL s^{-1})
f_c	caudal fin-beat frequency (Hz)
f_p	pectoral fin-beat frequency (Hz)
$\dot{M}_{O_2}$	oxygen consumption rate (mg O$_2$ kg^{-1} h^{-1})
$\dot{M}_{O_2E}$	estimated oxygen consumption rate (mg O$_2$ kg^{-1} h^{-1})
T	fin-beat period (s)
T_E	estimated fin-beat period (s)
U	swimming speed (BL s^{-1})
$\overline{U}$	mean swimming speed (BL s^{-1})
U_{p-c}	gait transition speed to pectoral–caudal swimming (BL s^{-1})
U_{crit}	critical swimming speed (BL s^{-1})

routinely subjected to wind-driven water motion (Denny and Gaylord, 2010) and can harbour over 60% of fish species that use labriform swimming as a primary means of locomotion (Fulton, 2010). Currently, we do not know how unsteady flows affect the swimming performance and energetics of labriform swimming fishes in coastal habitats.

We used intermittent-flow respirometry to compare the energetics, swimming performance and kinematics of a marine labriform swimmer, the shiner surfperch (*Cymatogaster aggregata* Gibbons), holding station in steady versus unsteady water flows. Our unsteady flow treatments mimicked a repeatable, unilateral wave surge scenario (sinusoidal variations in water flow velocity in a single direction, around a constant mean velocity) with low- and high-amplitude fluctuations in flow velocity. These two treatments are hereafter referred to as low and high unsteady flow. The vertical component of orbital waves was absent from the flow changes imposed, which therefore mimicked the horizontal component of waves. This movement (i.e. parallel to the seabed) is the dominant flow for travelling waves in shallow, coastal waters (Denny, 2006; Webb et al., 2010).

First, we tested whether fish swimming in unsteady flows incur greater swimming costs than fish in steady flow at the same mean velocity. Second, we estimated the values of oxygen consumption rate ($\dot{M}_{O_2}$) for fish swimming in the two unsteady flow treatments using simulations based on the non-linear relationship between swimming speed (U) and $\dot{M}_{O_2}$ obtained in steady flow. Third, we compared observed ($\dot{M}_{O_2}$) and estimated ($\dot{M}_{O_2E}$) oxygen consumption rates, where their difference may result from additional costs of accelerating and decelerating as well as maintaining stability in unsteady flow. Finally, we examined whether observed differences in $\dot{M}_{O_2}$ between the three flow treatments were related to pectoral fin kinematics measured on different time scales (time-averaged over 300 s versus instantaneous over the duration of one fin beat cycle) and body movements in the swim chamber to understand possible mechanisms underlying differences in oxygen consumption rates.

RESULTS

Respirometry

The hydrodynamics-based power functions describing the $\dot{M}_{O_2}$–swimming speed relationship in the three flow treatments (Fig. 1) were:

Steady flow: $\dot{M}_{O_2} = 129.91 \pm 10.63 \times 4.56 \pm 2.39 U^{3.37 \pm 0.42}$, (1)

Low unsteady flow:
$$\dot{M}_{O_2} = 115.74 \pm 10.93 \times 9.78 \pm 4.45 U^{2.57 \pm 0.35}, \quad (2)$$

High unsteady flow:
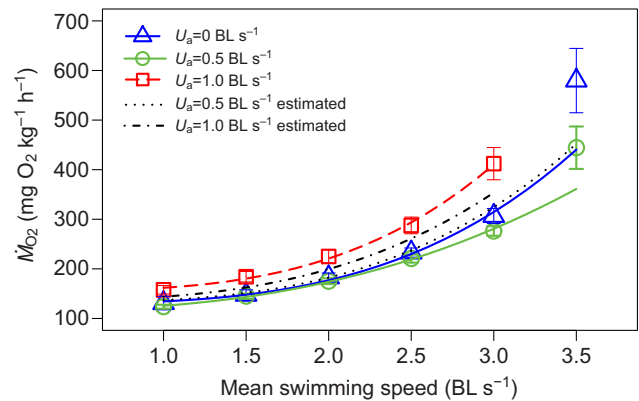$$\dot{M}_{O_2} = 155.44 \pm 20.10 \times 6.37 \pm 6.14 U^{3.36 \pm 0.84}. \quad (3)$$

Fig. 1. Observed and estimated oxygen consumption rates as a function of mean swimming speed. Oxygen consumption rate ($\dot{M}_{O_2}$; mg O$_2$ kg^{-1} h^{-1}) in relation to mean swimming speed for *Cymatogaster aggregata* in three water flow conditions: steady flow (U_a=0 BL s^{-1}; blue triangles), low-amplitude unsteady flow (U_a=0.5 BL s^{-1}; green circles) and high-amplitude unsteady flow (U_a=1.0 BL s^{-1}; red squares). $R^2_{LMM(m)}$=0.86 and $R^2_{LMM(c)}$=0.90. Error bars are ±1 s.e.m. Relationships are based on aerobic swimming (i.e. $\dot{M}_{O_2}$ measurements at speeds that did not induce bursting-and-coasting). The black dotted and dot-dashed lines indicate estimated oxygen consumption rates ($\dot{M}_{O_2E}$) for fish in low- and high-amplitude unsteady flow, respectively. $\dot{M}_{O_2E}$ was calculated by integrating a sinusoidal function based on experimental variations in flow speed (period of 5 s, amplitude of 0.5 or 1 BL s^{-1}) into the equation for the $\dot{M}_{O_2}$–swimming speed relationship in steady flow (see Materials and methods, and Fig. 7). U_a, amplitude of flow velocity fluctuations.

There were no significant differences in the shape of the relationship among flow treatments (LMM, quadratic term × treatment interaction, contrast group=steady flow, both $P>0.10$; Fig. 1). The linear coefficient (which shifts the axis of symmetry away from the y-axis) of the $\dot{M}_{O_2}$–swimming speed relationship in steady flow differed from that of the low (LMM, $t=-2.1$, $P=0.04$) and high unsteady flow treatments (LMM, $t=3.5$, $P<0.001$; Fig. 1). Importantly, fish in high unsteady flow had consistently higher oxygen consumption rates than fish in steady flow by 25.3% on average (range 20.5–34.4%; LMM, $t=4.3$, $P<0.001$; Fig. 1). Fish swimming in the low unsteady flow treatment consumed on average 8.3% (range 1.8–23.3%) less oxygen than fish in steady flow, but this difference was not significant (LMM, $t=-1.25$, $P=0.23$; Fig. 1).

Calculations of $\dot{M}_{O_2E}$ indicated that fish swimming in the low unsteady flow treatment should consume on average 2.75% (range 1.63–3.1%) more oxygen than fish in steady flow, whereas fish in high unsteady flow should consume on average 11.1% more (range 6.7–13.3%; Fig. 1). Observed $\dot{M}_{O_2}$ did not differ significantly from $\dot{M}_{O_2E}$ for fish in low unsteady flow (LMM, $t=-1.76$, $P=0.08$) but was significantly higher than $\dot{M}_{O_2E}$ for fish in high unsteady flow (LMM, $t=2.05$, $P=0.04$; Fig. 1).

Swimming performance

Fish in the different flow treatments transitioned from a pectoral to a pectoral–caudal swimming gait (U_{p-c}) at different swimming speeds (ANOVA, $F_{2,17}=7.18$, $P<0.01$; Fig. 2). Fish in high unsteady flow reached U_{p-c} at lower swimming speeds than fish in steady flow (Tukey's HSD, $P<0.05$) and in low unsteady flow (Tukey's HSD, $P<0.01$; Fig. 2). There was no difference in U_{p-c} between fish in low unsteady and steady flow (Tukey's HSD, $P=0.85$). Critical swimming speed was also different among treatments (ANOVA, $F_{2,17}=3.87$, $P<0.05$). Fish in high unsteady flow reached U_{crit} at lower swimming speeds than fish in low unsteady flow (Tukey's
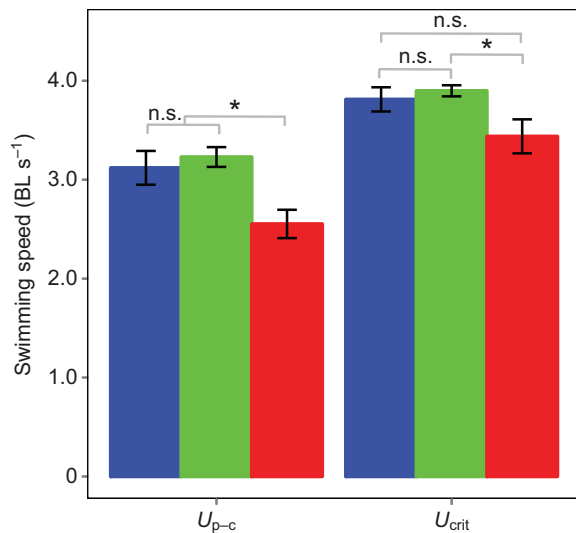
Fig. 2. *Cymatogaster aggregata* swimming performance in three flow treatments. Swimming performance of *C. aggregata* in steady flow (blue bars), low unsteady flow (U_a=0.5 BL s^{-1}; green bars) and high-amplitude unsteady flow (U_a=1.0 BL s^{-1}; red bars). U_{p-c}, gait transition speed (fish transition to caudal-assisted pectoral swimming); U_{crit}, critical (or maximum) swimming speed. Error bars are ±1 s.e.m. Asterisks denote significance (*$P<0.05$); n.s., not significant.

HSD, $P<0.05$). The U_{crit} of fish in steady flow did not differ from that in either high (Tukey's HSD, $P=0.13$) or low (Tukey's HSD, $P=0.88$) unsteady flow.

Time-averaged fin-beat frequency

Pectoral fin-beat frequency (f_p) increased with swimming speed (LMM slope, $F_{1,79}=392.9$, $P<0.001$) in a similar fashion for all three flow treatments (LMM interaction, $F_{1,79}=0.78$, $P=0.46$; Fig. 3A). In turn, f_p was a good predictor of oxygen consumption rates in all three treatments (LMM slope, $F_{1,79}=315.6$, $P<0.001$; LMM interaction, $F_{2,79}=0.07$, $P>0.90$; Fig. 3B), but fish in high unsteady flow consistently consumed more oxygen for a given f_p than fish in either steady or low unsteady flow (LMM intercept; $F_{2,16}=6.55$, $P<0.01$; Fig. 3B).

Instantaneous fin-beat period

Pectoral fin-beat period (T) decreased with swimming speed (LMM slope, $F_{1,79}=931.1$, $P<0.001$) similarly for fish in all three flow treatments (LMM interaction, $F_{2,79}=1.07$, $P=0.35$). However, variation (CV) in T across swimming speeds differed among flow treatments and increased with the degree of flow unsteadiness (Fig. 4). Observed variations in T were consistently higher than the estimated variation (T_E) for fish in high unsteady flow, but not for fish in low unsteady flow (Fig. 4). There was a significant overall negative association between variation in T and $\dot{M}_{O_2}$ (LMM slope, $F_{1,14}=66.0$, $P<0.001$) for fish in high unsteady flow and the slope of this relationship did not differ among swimming speeds (LMM interaction, $F_{3,14}=0.18$, $P=0.91$; Fig. 5B). The 95% confidence interval of the estimates for both the within-speed slope (estimate=−0.261, 95% CI=−0.400 to −0.122) and between-speed slope (estimate=−0.556, 95% CI=−0.930 to −0.182) did not overlap zero, indicating that these slopes differed from zero. In contrast, associations between variation in T and $\dot{M}_{O_2}$ were generally non-significant and inconsistent across swimming speeds for fish in low unsteady flow (Fig. 5A). The 95% confidence interval for the estimate of the between-speed slope did not overlap zero (estimate=−0.997, 95% CI=−1.516 to −0.478); however, the
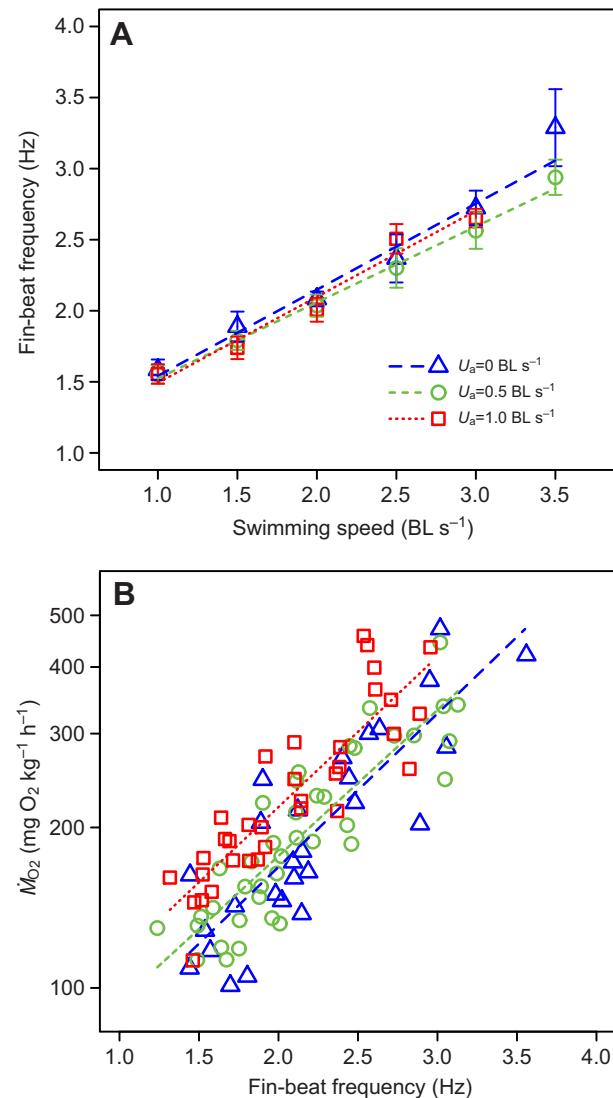

Fig. 3. Relationships between pectoral fin-beat frequency, swimming speed and oxygen consumption rate. (A) Pectoral fin-beat frequency (f_p) in relation to swimming speed [$R^2_{LMM(m)}$=0.77; $R^2_{LMM(c)}$=0.81], and (B) oxygen consumption rate ($\dot{M}_{O_2}$; log scale) in relation to fin-beat frequency [$R^2_{LMM(m)}$=0.76; $R^2_{LMM(c)}$=0.79] for *C. aggregata* swimming in steady flow (blue triangles), low unsteady flow (0.5 BL s^{-1}; green circles) and high-amplitude unsteady flow (1.0 BL s^{-1}; red squares). U_a, amplitude of flow velocity fluctuations.

within-speed slope estimate overlapped zero (estimate=−0.154, 95% CI=−0.340 to 0.032), indicating that variation in T had no effect on $\dot{M}_{O_2}$.

Body movement

There was a significant overall negative association between fish displacement (horizontal and vertical body movement) and variation in T (LMM slope, $F_{1,14}=7.16$, $P=0.02$) for fish in high unsteady flow, and the slope of this relationship did not differ among swimming speeds (LMM interaction, $F_{3,14}=0.20$, $P=0.89$; Fig. 6).

DISCUSSION

Swimming performance and oxygen consumption

Many labriform fishes live in marine environments and experience variable speed flows created by travelling waves in inshore
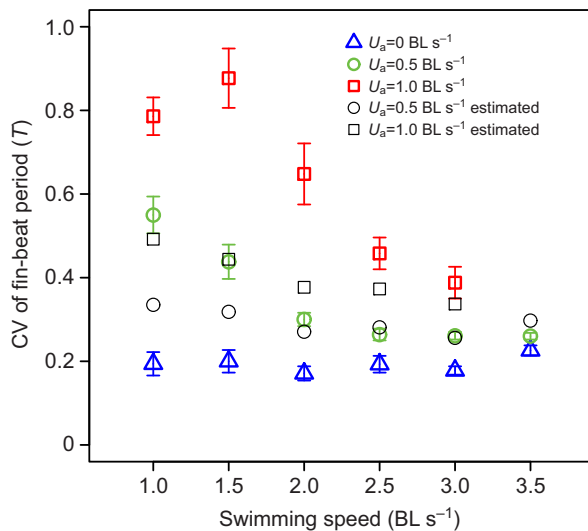
Fig. 4. Observed and estimated variation in pectoral fin-beat period. Mean variation (CV) in pectoral fin-beat period (T) within a 5 s wave period in relation to swimming speed for *C. aggregata* in steady flow (U_a=0 BL s^{-1}; blue triangles), low unsteady flow (U_a=0.5 BL s^{-1}; green circles), and high unsteady flow (U_a=1.0 BL s^{-1}; red squares). Black circles and squares represent the estimated variation in fin-beat period for low- and high-amplitude unsteady flow, respectively. Estimated variations were adjusted by adding the background variations in T observed for fish in steady flow (i.e. values represented by the blue triangles). U_a, amplitude of flow velocity fluctuations.

Fig. 5. Effect of variation in pectoral fin-beat period on oxygen consumption rate. Oxygen consumption rate ($\dot{M}_{O_2}$; log$_{10}$ scale) in relation to variation in pectoral fin-beat period within a 5 s wave cycle for individual *C. aggregata* swimming (A) at five different speeds (1.0, 1.5, 2.0, 2.5 and 3.0 BL s^{-1}) in low-amplitude (U_a=0.5 BL s^{-1}) unsteady flow and (B) at four different speeds (1.0, 1.5, 2.0 and 2.5 BL s^{-1}) in high-amplitude (U_a=1.0 BL s^{-1}) unsteady flow [$R^2_{LMM(m)}$=0.81; $R^2_{LMM(c)}$=0.90]. Data are shown for swimming speeds that induced only aerobic metabolism and pectoral fin swimming exclusively (i.e. below U_{p-c}).

habitats. Our experimental flow treatments mimicked unidirectional wave surge with either low- or high-amplitude velocity fluctuations and a period of 5 s, similar to waves in Puget Sound, Washington (Finlayson, 2006). We found that high unsteady flow tended to decrease fish swimming performance (Fig. 2) and increase swimming costs by an average of 25.3% compared with steady flow (Fig. 1). This increase in oxygen consumption rate also exceeded the 11.1% average increase expected based on calculations of $\dot{M}_{O_2E}$ (i.e. $\dot{M}_{O_2}$ estimated using the non-linear relationship between swimming speed and $\dot{M}_{O_2}$ in steady flow) (Fig. 1). Together, these results suggest that estimates of fish swimming energetics based on steady flow conditions underestimate the costs of swimming in water flow with large velocity fluctuations (in the order of one body length). This discrepancy may be due to additional energy expenditure from fish accelerating and decelerating (see Kramer and McLaughlin, 2001; Minetti et al., 2001) as well as correcting for postural disturbances (see Webb, 2006; Webb et al., 2010) to maintain their position and stability during flow velocity changes. In contrast, swimming performance and oxygen consumption rates did not increase in low unsteady flow relative to steady flow. This result is consistent with the small estimated increase in oxygen consumption rate of only 2.75%, on average, based on $\dot{M}_{O_2E}$. Further experiments are necessary to establish the relative costs of maintaining stability and varying acceleration for fish swimming in unsteady flows.

Spatial and/or temporal fluctuations in water flow velocity can result in both energetic challenges and benefits for fishes (Lacey et al., 2012). Enders et al. (Enders et al., 2003) found that juvenile Atlantic salmon, *Salmo salar*, incurred higher energetic costs even at relatively low water velocity fluctuations in turbulent flow compared with laminar flow. In contrast, other studies have shown that BCF swimmers can exploit vortices that have an element of predictability: by bending their body around vortices, fish can
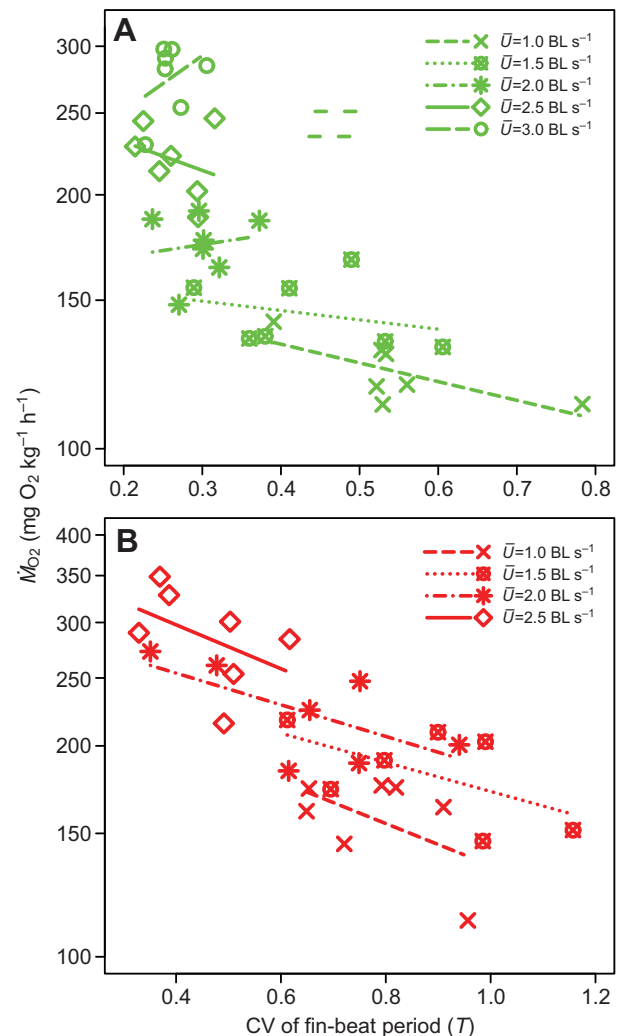
generate forward thrust with less energy expenditure (e.g. Liao et al., 2003b; Taguchi and Liao, 2011). Our results support the general finding that disturbances from flow variations are important only if they are large relative to the size of the fish (Pavlov et al., 2000; Lupandin, 2005; Liao, 2007; Tritico and Cotel, 2010; Webb et al., 2010); irrespective of its mean swimming speed, *C. aggregata* appeared unaffected by relatively small water velocity fluctuations of 0.5 BL s^{-1} while experiencing significantly higher energetic demands when subjected to larger fluctuations of 1 BL s^{-1}.

Time-averaged pectoral fin kinematics and oxygen consumption

The relationship between mean swimming speed and pectoral fin-beat frequency (measured over 300 s) did not differ among flow treatments (Fig. 3A). Despite these similarities, for a given fin-beat frequency, fish in high unsteady flow consumed significantly more
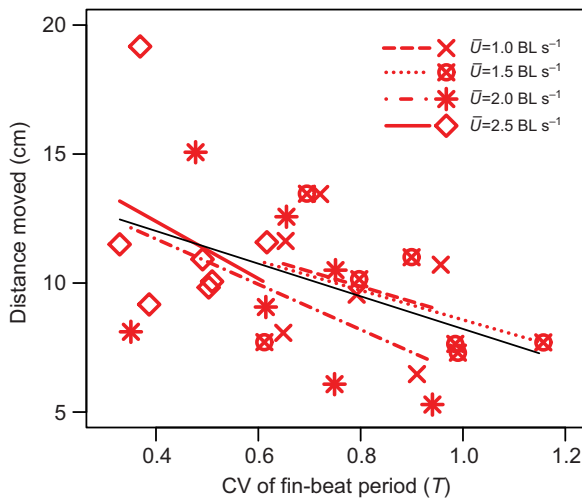
Fig. 6. Effect of variation in fin-beat period on distance moved in the swim chamber. Distance moved (cm) in relation to variation (CV) in pectoral fin-beat period within a 5 s wave cycle for individual *C. aggregata* swimming at four different speeds (1.0, 1.5, 2.0 and 2.5 BL s^{-1}) in high-amplitude (U_a=1.0 BL s^{-1}) unsteady flow. $R^2_{LMM(m)}$=0.17 and $R^2_{LMM(c)}$=0.64. Data are shown for swimming speeds that resulted only in aerobic activity (i.e. swimming speeds that induced burst-and-coast swimming are excluded). Regression lines show relationships within the four distinct high-amplitude swimming speeds; the overall relationship is shown as a solid black line.

oxygen than fish in both low unsteady and steady flow (Fig. 3B). This suggests that a time-averaged measure of fin use is independent of observed differences in $\dot{M}_{O_2}$. Within a given 5 s period of water velocity fluctuations, we observed individuals in low and high unsteady flows altering their fin-beat movements: fish were beating their fins less frequently as the flow velocity decreased and, conversely, increased their fin-beat frequency as the flow velocity increased (see supplementary material Movie 1). Despite these adjustments in fin kinematics, the mean fin-beat frequency (f_p) was the same at any given mean swimming speed, regardless of the flow treatment. Because f_p was calculated as the average number of fin beats over a time scale of minutes, this time-averaged measure of fin use did not capture adjustments in the timing of fin beats made by fishes in unsteady flow. Therefore, measurements of fin kinematics on a shorter time scale are needed to explain differences in $\dot{M}_{O_2}$ among treatments (see below, Variation in instantaneous pectoral fin kinematics).

Pectoral fin-beat frequency is positively related to swimming speed and/or oxygen consumption in several species of labriform fishes (e.g. Mussi et al., 2002; Kendall et al., 2007; Tudorache et al., 2009; Johansen et al., 2010). Some authors have suggested that the relationships between fin-beat frequency, oxygen consumption rate and swimming speed in a given fish species may provide useful indicators of swimming energetics in the wild, which are extremely difficult to estimate in aquatic species (Steinhausen et al., 2005; Ohlberger et al., 2007; Tudorache et al., 2009; Layton, 2011). However, our results suggest that the use of time-averaged fin kinematics to predict oxygen consumption rates depends on the hydrodynamic context in which these estimates are made. As such, caution is warranted when inferring oxygen consumption rates from time-averaged measures of fin-beat frequency.

Variation in instantaneous pectoral fin kinematics
Although time-averaged f_p was similar across flow treatments, fin-beat period (T) clearly differed. The consistently timed beats of

fish swimming in steady flow resulted in low variation in T, whereas the rapid speeding up and slowing down of fin beats in unsteady flow resulted in higher variations in T (Fig. 4). As mean swimming speed increases, fish must beat their fins faster in order to keep up with increasing flow speed, resulting in a shorter refractory or gliding period between fin beats. As a result, both the observed and predicted variation in T decreased with increasing swimming speed for fish in the unsteady flow treatments (Fig. 4). In contrast, variation in T remained constant in steady flow (Fig. 4), despite increases in f_p with higher swimming speeds (Fig. 3A).

In low unsteady flow, observed variations in T were greater than the estimated variation (T_E) only at low swimming speeds, where water velocity fluctuations would have had a minimal effect on fish (Fig. 4). In high unsteady flow, however, observed variations in T were consistently greater than estimated variations, across all swimming speeds (Fig. 4). These differences in fin-beat period variability between treatments are consistent with observed differences in $\dot{M}_{O_2}$ (Fig. 1).

Similarly, there was a clear relationship between $\dot{M}_{O_2}$ and variation in T in high unsteady flow (Fig. 5B) but not in low unsteady flow (Fig. 5A): fish with greater variation in T consumed less oxygen for a given mean swimming speed in high unsteady flow (Fig. 5A). While we did not quantify whether, within one 5 s wave period, accelerations in water velocity coincided with shorter fin-beat periods and vice versa, these relationships clearly indicate that larger variations in T were energetically advantageous in conditions of high flow variability. This also suggests that some fish are capable of adjusting the duration of their fin beats in response to changes in water flow velocity to maintain a relatively constant ground speed in the swim chamber (Fig. 6). Specifically, by increasing the refractory period of fin beats as the water decelerates, fish may be able to conserve energy by increasing their glide towards the end of the wave cycle. Fish with lower variation in T may not take advantage of decelerations in water flow velocity and may resort to more energetically costly behaviours to try and maintain their position in the swim chamber. Such behaviours were not assessed in this study but could include modifying the amplitude and/or the power output of fin strokes to accelerate and overcome resistance at various swimming speeds, as well as braking to control posture and position during deceleration.

In conclusion, our results suggest that swimming costs in unsteady flows depend on the magnitude of the water velocity fluctuations. When velocity fluctuations were relatively large, the energetic costs of swimming in unsteady flow exceeded the costs of swimming in steady flow at the same mean velocity. It is important to note that these costs apply to station-holding fishes, which swim to remain stationary relative to the substrate. In contrast, travelling fishes exposed to wave surge might be able to conserve energy by taking advantage of forward surges and varying their ground speed while maintaining a constant velocity relative to the water. Our results are also conservative because hydrodynamic perturbations in our experiments were unidirectional and designed to minimize turbulence. Coastal habitats are often characterized by turbulent, oscillatory wave-driven water motion, which may require fishes to expand more energy for postural control and stability. Swimming costs also depend on the ability of individual fish to adjust their fin kinematics to the flow environment and avoid displacement while station holding in the swim chamber. Individual variability in swimming performance has previously been observed in a number of species and has been shown to be both repeatable and

biologically important (Kolok, 1999). It is possible that inter-individual differences in our study relate to differences in habitat use among fish; for example, individuals foraging high in the water column may experience greater water flows than individuals that remain closer to the substrate. Further studies should examine the learning potential of individual fish to modify their fin-beat kinematics via repeated exposure to variable water flows.

MATERIALS AND METHODS
Fish collections and husbandry
Adult *Cymatogaster aggregata* were collected using a beach seine net at Fourth of July and Jackson's Beach on San Juan Island, Washington, USA, in August 2011. Fish were held in flow-through aquaria at the University of Washington's Friday Harbor Laboratories at an ambient light regime. Tanks were continuously supplied with filtered seawater (salinity 34 ppt) at a mean temperature of 12°C (range 11 to 13°C). Given the proximity of the laboratory to the collection site, fish were not fed and were tested shortly after their capture, ensuring near-wild conditions during the experiments. Fish were fasted for a minimum of 24 h before the experimental trials to ensure that satiation was standardized across individuals (Niimi and Beamish, 1974; Johansen et al., 2010; Roche et al., 2013). The experimental protocol was approved by the University of Washington in accordance with Institutional Animal Care and Use Committee standards (IACUC permit no. 4238-04).

Respirometry
We measured oxygen consumption rates ($\dot{M}_{O_2}$; mg O_2 kg^{-1} h^{-1}) for 20 fish (total length=14.84±0.49 cm; mass=46.3±6.3 g; means ± s.d.) swimming in an 8.31 litre clear Plexiglas Steffensen-type respirometer (Steffensen et al., 1984; Methling et al., 2011) with a working section of 9.0×26.0×10.0 cm (width×length×depth) (supplementary material Fig. S1). Oxygen levels in the respirometer were recorded using a fibre optic oxygen meter (PreSens Fibox 3, Regensburg, Germany) monitored with AutoResp V1 (Loligo Systems, Copenhagen, Denmark). We calibrated the flow in the working section of the respirometer from 0 to 80±0.5 cm s^{-1} (mean ± s.e.m.) using a digital TAD W30 flow meter (Höntzsch, Waiblingen, Germany) at 1 cm intervals. The flow velocity profile varied less than 5% across the full cross-section of the working chamber and we did not observe fish favouring one corner or particular side of the working section during the swim trials. Changes in flow speed inside the swim chamber can lag behind changes in the rotational speed of the propeller; however, we measured flow velocity during oscillations in propeller speed and observed minimal dampening and attenuation of intended flow speed minima/maxima in the swim chamber. Solid blocking effects of the fish were corrected by the respirometry software (AutoResp V1); the mean fish cross-sectional area was 8.1% of the swim chamber cross-sectional area, corresponding to a 3.5–4% greater effective water velocity around the fish compared with the water velocity in the empty swim chamber (Webb, 1975). We used UV filtration to reduce bacterial growth in the system and regularly rinsed the respirometer in freshwater to ensure that bacterial respiration rates remained below 15% of the standard metabolic rate of fish. Three $\dot{M}_{O_2}$ determinations were run without fish before and after each trial to measure bacterial respiration in the test chamber. Background respiration rates were determined from the slope of the linear regression between initial and final measurements of background respiration rates and subtracted from each $\dot{M}_{O_2}$ determination.

At the start of a trial, fish were placed in the respirometer and left to acclimate for 6 to 8 h at a swimming speed of 0.5 BL s^{-1} until their oxygen consumption rate stabilized. This speed corresponded to the lowest water flow necessary to ensure constant swimming and minimize spontaneous activity. Using six of the 20 test subjects, we measured $\dot{M}_{O_2}$ as a function of steady swimming speed (*U*) starting at 1.0 BL s^{-1} and increasing flow speed by increments of 0.5 BL s^{-1} every 30 min, following a standard critical swimming speed (*U*$_{crit}$) protocol (Brett, 1964; Plaut, 2001). $\dot{M}_{O_2}$ was calculated by the respirometry software (AutoResp V1) as the slope of the linear regression of oxygen concentration decline over time for each determination cycle using the equation:

$$\dot{M}_{O_2} = sV_{resp}\alpha M^{-1}, \qquad (4)$$

where *s* is the slope (mmHg h^{-1}), V_{resp} is the volume of the respirometer minus the volume of the fish (l), α is the solubility of oxygen in water (μg O_2 l^{-1} $mmHg^{-1}$) adjusted for temperature and barometric pressure and *M* is the mass of the fish (kg). $\dot{M}_{O_2}$ was determined every 10 min following a 225 s flush, 75 s wait and 300 s measure cycle. The trial stopped when fish could no longer swim unassisted or were forced to rest on the back grid of the flow chamber for ≥5 s. Both time and speed at this occurrence were recorded and the water flow was reduced to 0.5 BL s^{-1}. The fish was then removed from the test chamber and returned to its holding tank.

We repeated the same step-wise procedure for the remaining 14 test subjects, but varied flow velocity by an amplitude of either 0.5 BL s^{-1} (low unsteady flow; *N*=7) or 1.0 BL s^{-1} (high unsteady flow; *N*=7) around the mean at each speed increment (e.g. 1.0±0.5 BL s^{-1}). These velocity fluctuations were adjusted for each individual fish based on body length, and approximated natural, wave-induced changes in flow speed on the coasts of Puget Sound [0–50 cm s^{-1} (Finlayson, 2006)]. We used a computer-generated sine function with a period of 5 s (TracerDAQ Pro, Measurement Computing, Norton, MA, USA) to create repeatable variations in water flow speed by continuously controlling the voltage to the motor and the rotational speed of the propeller in the respirometer. Five seconds corresponds to moderate wave periods in the San Juan Islands (Finlayson, 2006). The computer was connected to a motor controller (Movitrac AC VFD, SEW Eurodrive, Lyman, SC, USA) via a USB-1208 ADDA converter (USB DAQ Data Acquisition, Measurement Computing). Flow straighteners were used to dissipate gross turbulence and produce flow with uniform micro-turbulence (Beamish, 1978). Eliminating micro-turbulence in flumes is practically impossible (Beamish, 1978); however, very small orbits with diameters much smaller than a fish's body length are unlikely to have notable effects on swimming performance (see Tritico and Cotel, 2010; Webb et al., 2010). We used flow visualization with neutrally buoyant particles (expandable polystyrene beads diameter <1 mm, Foamex Polystyrene, Revesby, Australia) in a similar respirometer to confirm the absence of large vortices. Given their small size, these particles allowed us to detect perturbations greater than 1 mm. Flow visualizations were filmed in high definition at 30 frames s^{-1}. Frame-by-frame measurements using the plugin MtrackJ in ImageJ (Meijering et al., 2012) revealed a relatively uniform flow profile and the absence of vortices with a diameter >0.5 cm (most were much smaller or almost nil), both in steady and unsteady flow conditions. Examples of flow characterizations in steady and high unsteady flow are provided in supplementary material Figs S2, S3, Table S1.

A computer-generated sine function that determined the rotational speed of the swim tunnel's propeller allowed us to precisely control four key parameters in the different flow conditions: the period, amplitude and wavelength of the water velocity fluctuations, and the mean flow velocity. Prior to the experiments, we calibrated the voltage from the computer-generated sine function with changes in water velocity in unsteady flow using a digital Höntzsch TAD W30 flow meter (Höntzsch, Waiblingen, Germany). We increased the mean water flow velocity from 1 to 4.5 BL s^{-1} by increments of 0.5 BL s^{-1}, following a standard U_{crit} protocol. The period was 5 s for all treatments and the amplitude varied between 0, 0.5 and 1 BL s^{-1} depending on the treatment. The wavelength varied between 5 BL and 22.5 BL because wavelength is a product of the period and the water flow velocity. The variance in water flow velocity was 0 for steady flow, 0.125 for low unsteady flow and 0.5 for high unsteady flow. The variance remained the same within each flow treatment as the amplitude of water velocity fluctuations was identical within treatment, across all mean swimming speeds. There was only small variation in the maximum and minimum flow velocities recorded around a given mean flow velocity, which indicated that the flow conditions were consistent (supplementary material Fig. S2, Table S1).

We used the hydrodynamics-based power function to describe the relationship between $\dot{M}_{O_2}$ and *U* in the different flow treatments (Wu, 1977; Videler, 1993):

$$\dot{M}_{O_2} = a + bU^c, \qquad (5)$$

where *a* is the estimated $\dot{M}_{O_2}$ at zero speed (standard metabolic rate; SMR), *b* is the linear coefficient and *c* is the exponent, which is indicative of aerobic swimming efficiency (Wardle et al., 1996). A three-parameter power or exponential function is preferred over a simpler, two parameter function

($\dot{M}_{O_2}=a10^{bU}$) for comparing swimming costs among groups when SMR is not measured directly (Roche et al., 2013). We restricted these analyses to aerobic swimming by excluding data for individual fish at swimming speeds that induced burst-and-coast swimming (see Korsmeyer et al., 2002; Svendsen et al., 2010). Burst-and-coast swimming was defined as an event that included caudal fin beats (1, 2 or 3 beats) and a subsequent forward glide motion >5 cm relative to a fixed point in the swim chamber, without the use of pectoral fins (see Svendsen et al., 2010).

Swimming performance

We used a Canon Vixic HV30 to video the test subjects continuously during each trial and determine their pectoral–caudal gait transition speed (U_{p-c}) and U_{crit}. A mirror was placed at 45 deg adjacent to the working section to record the top and side view of the fish in a single frame. U_{p-c} was reached when fish recruited their caudal fin to assist pectoral fin swimming more than once in 5 s (caudal fin-beat frequency, f_c>0.2 Hz); U_{crit} was reached when fish could no longer swim unassisted and were forced to rest on the back grid of the working section of the respirometer for more than five consecutive seconds (Johansen and Jones, 2011). We calculated U_{p-c} and U_{crit} following the equation in Brett (Brett, 1964):

$$U_{p-c} \text{ or } U_{crit} = U + U_i \times (t/t_i), \tag{6}$$

where U is the penultimate swimming speed before the fish changed gait from pectoral to pectoral–caudal swimming (U_{p-c}) or before the fish fatigued and stopped swimming (U_{crit}); U_i is the swimming speed at which the fish changed swimming gait or was unable to continue swimming (i.e. swimming speed at increment i); t is the length of time the fish swam at the final swimming speed where gait change or fatigue occurred; and t_i is the amount of time fish were swam at each speed interval in the trial (30 min).

Fin-beat kinematics (frequency and period) and body movement

For each fish ($N=20$) and each speed increment, we examined the three 5 min video segments that corresponded to the $\dot{M}_{O_2}$ measurement cycles. Using ODlog (Macropod Software), we recorded the number of (1) pectoral fin beats, (2) combinations of pectoral and caudal fin beats and (3) caudle fin beats that resulted in burst-and-coast swimming. We calculated pectoral fin-beat frequency (f_p) in Hz as the number of pectoral fin beats performed divided by the time elapsed during the analysis period (300 s). Calculated in this way, fin-beat frequency represents a time-averaged measure of fin oscillations (Drucker and Jensen, 1996).

To examine finer-scale effects of water speed fluctuations on pectoral fin kinematics, we measured the period of individual pectoral fin beats (T) during the 5 s cycle of sinusoidal water velocity fluctuations. We used field-by-field video analysis to record values of T three times per fish (once per $\dot{M}_{O_2}$ determination) at each swimming speed. Fin-beat period is the duration of a pectoral fin-beat cycle, which begins and ends with consecutive onsets of pectoral fin abduction (Drucker and Jensen, 1996). It includes both the propulsive phase measured from the onset of abduction to the end of adduction, and a non-propulsive phase during which the fish glides until the onset of the next abduction (Drucker and Jensen, 1996). We calculated the mean and the coefficient of variation (CV; s.d./mean) of fin-beat period across the three $\dot{M}_{O_2}$ determinations for each fish and swimming speed. Because there was considerable individual level variation in oxygen consumption rates and fin-beat period among fish in high unsteady water flow (see Results), we tested whether fish that had a high variation in fin-beat period (i.e. longer and shorter fin-beat cycles as denoted by the CV of fin-beat period) in response to high fluctuations in water flow velocity consumed less oxygen than fish that had less variable fin-beat periods (see supplementary material Movie 1). We also tested whether these fish were better able to hold station in the swim chamber by maintaining their ground speed constant. We used field-by-field video analysis to measure horizontal and vertical body displacements during the 5 s cycle of sinusoidal water velocity fluctuation three times per fish (once per $\dot{M}_{O_2}$ determination) at each swimming speed.

Estimated oxygen consumption and fin-beat period

In fishes, the response curve of oxygen consumption rate versus swimming speed is a positive, nonlinear function (e.g. Korsmeyer et al., 2002; Cannas
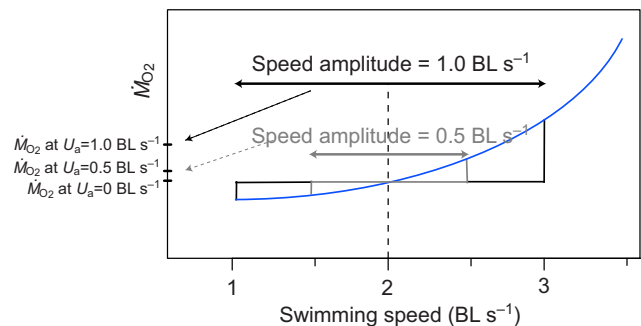
Fig. 7. Theoretical effects of sinusoidal variations in water flow velocity (or swimming speed) around a constant mean speed (2 BL s^{-1} in this example, indicated by a dashed vertical line) on oxygen consumption rate ($\dot{M}_{O_2}$). Because this relationship is nonlinear, increases in $\dot{M}_{O_2}$ from swimming at speeds above the mean outweigh decreases in $\dot{M}_{O_2}$ from swimming below the mean. These effects are greater for large (1 BL s^{-1}) than small (0.5 BL s^{-1}) amplitude variations in water flow speed. U_a, amplitude of flow velocity fluctuations.

et al., 2006); therefore, for the same mean swimming speed, fish experiencing cyclic changes in water flow velocity should consume more oxygen than fish swimming at a constant velocity (Fig. 7) (see Ruel and Ayres, 1999). To compare observed and estimated oxygen consumption rates, we calculated estimated changes in $\dot{M}_{O_2}$ values ($\dot{M}_{O_2E}$) as a function of swimming speed for the low and high unsteady flow treatments. This was achieved by integrating a sinusoidal function based on experimental variations in flow speed (period of 5 s, amplitude of 0.5 or 1 BL s^{-1}) into the equation for the $\dot{M}_{O_2}$–swimming speed relationship in steady flow. Comparisons of $\dot{M}_{O_2}$ and $\dot{M}_{O_2E}$ values allowed us to determine whether potential differences could be attributed to factors other than the mathematical properties (i.e. non-linearity) of the swimming speed–$\dot{M}_{O_2}$ relationship. Such factors could include costs associated with stability and acceleration–deceleration. We used this same procedure to calculate the variation (CV) in estimated fin-beat period (T_E) as a function of swimming speed, based on the relationship between swimming speed and fin-beat frequency in steady flow. In steady flow, we considered variability in pectoral fin-beat period to be the natural amount of variation for individuals swimming in our flow chamber; therefore, we adjusted the CV of T_E for fish in the two unsteady flow treatments by adding the background variations in fin-beat period observed for fish in steady flow.

Statistical analysis

We used a general linear mixed effects model (LMM; lme function in R) to test for differences in the $\dot{M}_{O_2}$–swimming speed relationship across flow treatments. We specified the relationship between speed and $\dot{M}_{O_2}$ as a second-degree polynomial and individual fish as a random effect. Mixed models are useful as they control for temporal autocorrelation among data points in physiological response curves (Peek et al., 2002; Bolker et al., 2009; Nakagawa et al., 2013). This same model was used to test for differences between estimated ($\dot{M}_{O_2E}$) and observed $\dot{M}_{O_2}$ values in the two unsteady flow treatments. We tested for differences in swimming performance (U_{p-c}, U_{crit}) across flow treatments with two one-way ANOVAs and subsequent Tukey's honestly significant difference (HSD) tests. We used five distinct LMMs with fish as a random factor to examine: (1) differences in the relationship between swimming speed and pectoral fin-beat frequency across flow treatments, (2) the relationship between pectoral fin-beat frequency and $\dot{M}_{O_2}$ across flow treatments, (3) the relationship between swimming speed and pectoral fin-beat period, (4) whether individual variation in fin-beat period explained differences in $\dot{M}_{O_2}$ for fish swimming in the low and high unsteady flow treatments, and (5) the relationship between variation in fin-beat period and fish displacement (i.e. body movement) in high unsteady flow. We specified random intercepts and a first-order autoregressive covariance structure to account for equally spaced points in time. Where needed, we used log$_{10}$ and exponential transformations

to linearize the data and meet the assumptions of normality and homoscedasticity. For mixed effects models, we determined $R^2_{LMM(m)}$, the proportion of variance explained by fixed factors, and $R^2_{LMM(c)}$, the proportion of variance explained by both fixed and random factors (Nakagawa et al., 2013). $R^2_{LMM(m)}$ values were almost identical to overall R^2 obtained for linear (non-mixed) models. We used within-group centring to compare estimates of within-group slope versus between-group slope and test relationships between variation in fin-beat period and $\dot{M}_{O_2}$ (van de Pol and Wright, 2009). All analyses were conducted in Rv2.11.1 (R Development Core Team, 2010). Data are deposited in figshare (public data repository, http://dx.doi.org/10.6084/m9.figshare.789064).

Supplementary material
Supplementary material available online at
http://jeb.biologists.org/lookup/suppl/doi:10.1242/jeb.085811/-/DC1

References

Arnold, S. J. (1983). Morphology, performance and fitness. *Am. Zool.* **23**, 347-361.

Beal, D. N., Hover, F. S., Triantafyllou, M. S., Liao, J. C. and Lauder, G. V. (2006). Passive propulsion in vortex wakes. *J. Fluid Mech.* **549**, 385-402.

Beamish, F. W. H. (1978). Swimming capacity. In *Fish Physiology*, Vol. 7 (ed. W. S. Hoar and D. J. Randall), pp. 101-187. New York, NY: Academic Press.

Bellwood, D. R. and Wainwright, P. C. (2001). Locomotion in labrid fishes: implications for habitat use and cross-shelf biogeography on the Great Barrier Reef. *Coral Reefs* **20**, 139-150.

Boisclair, D. and Sirois, P. (1993). Testing assumptions of fish bioenergetics models by direct estimation of growth, consumption, and activity rates. *Trans. Am. Fish. Soc.* **122**, 784-796.

Bolker, B. M., Brooks, M. E., Clark, C. J., Geange, S. W., Poulsen, J. R., Stevens, M. H. H. and White, J.-S. S. (2009). Generalized linear mixed models: a practical guide for ecology and evolution. *Trends Ecol. Evol.* **24**, 127-135.

Brett, J. R. (1964). The respiratory metabolism and swimming performance of young sockeye salmon. *J. Fish Res. Board Can.* **21**, 1183-1226.

Cannas, M., Schaefer, J., Domenici, P. and Steffensen, J. F. (2006). Gait transition and oxygen consumption in swimming striped surfperch *Embiotoca lateralis* Agassiz. *J. Fish Biol.* **69**, 1612-1625.

Claireaux, G., Webber, D., Kerr, S. and Boutilier, R. (1995). Physiology and behaviour of free-swimming Atlantic cod (*Gadus morhua*) facing fluctuating temperature conditions. *J. Exp. Biol.* **198**, 49-60.

Clark, T. D., Jeffries, K. M., Hinch, S. G. and Farrell, A. P. (2011). Exceptional aerobic scope and cardiovascular performance of pink salmon (*Oncorhynchus gorbuscha*) may underlie resilience in a warming climate. *J. Exp. Biol.* **214**, 3074-3081.

Cook, C. L. and Coughlin, D. J. (2010). Rainbow trout *Oncorhynchus mykiss* consume less energy when swimming near obstructions. *J. Fish Biol.* **77**, 1716-1723.

Denny, M. W. (2006). Ocean waves, nearshore ecology, and natural selection. *Aquat. Ecol.* **40**, 439-461.

Denny, M. W. and Gaylord, B. (2010). Marine ecomechanics. *Ann. Rev. Mar. Sci.* **2**, 89-114.

Drucker, E. and Jensen, J. (1996). Pectoral fin locomotion in the striped surfperch. I. Kinematic effects of swimming speed and body size. *J. Exp. Biol.* **199**, 2235-2242.

Enders, E. C., Boisclair, D. and Roy, A. G. (2003). The effect of turbulence on the cost of swimming for juvenile Atlantic salmon (*Salmo salar*). *Can. J. Fish. Aquat. Sci.* **60**, 1149-1160.

Enders, E. C., Boisclair, D. and Roy, A. G. (2005). A model of total swimming costs in turbulent flow for juvenile Atlantic salmon (*Salmo salar*). *Can. J. Fish. Aquat. Sci.* **62**, 1079-1089.

Farrell, A., Lee, C., Tierney, K., Hodaly, A., Clutterham, S., Healey, M., Hinch, S. and Lotto, A. (2003). Field-based measurements of oxygen uptake and swimming performance with adult Pacific salmon using a mobile respirometer swim tunnel. *J. Fish Biol.* **62**, 64-84.

Finlayson, D. P. (2006). *The Geomorphology of Puget Sound Beaches*. PhD thesis, School of Oceanography, University of Washington, Seattle, WA, USA.

Fulton, C. J. (2010). The role of swimming in reef fish ecology. In *Fish Locomotion: An Eco-Ethological Prespective* (ed. P. Domenici and B. G. Kapoor), pp. 374-406. Enfield, NH: Science Publishers.

Gaylord, B., Denny, M. W. and Koehl, M. A. (2008). Flow forces on seaweeds: field evidence for roles of wave impingement and organism inertia. *Biol. Bull.* **215**, 295-308.

Irschick, D. J. and Garland, T. (2001). Integrating function and ecology in studies of adaptation: investigations of locomotor capacity as a model system. *Annu. Rev. Ecol. Syst.* **32**, 367-396.

Johansen, J. L. and Jones, G. P. (2011). Increasing ocean temperature reduces the metabolic performance and swimming ability of coral reef damselfishes. *Glob. Chang. Biol.* **17**, 2971-2979.

Johansen, J. L., Vaknin, R., Steffensen, J. F. and Domenici, P. (2010). Kinematics and energetic benefits of schooling in the labriform fish, striped surfperch *Embiotoca lateralis*. *Mar. Ecol. Prog. Ser.* **420**, 221-229.

Kendall, J. L., Lucey, K. S., Jones, E. A., Wang, J. and Ellerby, D. J. (2007). Mechanical and energetic factors underlying gait transitions in bluegill sunfish (*Lepomis macrochirus*). *J. Exp. Biol.* **210**, 4265-4271.

Kolok, A. S. (1999). Interindividual variation in the prolonged locomotor performance of ectothermic vertebrates: a comparison of fish and herpetofaunal methodologies and a brief review of the recent fish literature. *Can. J. Fish. Aquat. Sci.* **56**, 700-710.

Korsmeyer, K. E., Steffensen, J. F. and Herskin, J. (2002). Energetics of median and paired fin swimming, body and caudal fin swimming, and gait transition in parrotfish (*Scarus schlegeli*) and triggerfish (*Rhinecanthus aculeatus*). *J. Exp. Biol.* **205**, 1253-1263.

Kramer, D. L. and McLaughlin, R. L. (2001). The behavioral ecology of intermittent locomotion. *Am. Zool.* **41**, 137-153.

Lacey, R., Neary, V. S., Liao, J. C., Enders, E. C. and Tritico, H. M. (2012). The ipos framework: linking fish swimming performance in altered flows from laboratory experiments to rivers. *River Res. Appl.* **28**, 429-443.

Layton, C. (2011). *Swimming Activities and Costs in Free-Living Coral Reef Wrasses* (Labridae). BSc Hons thesis, Research School of Biology, The Australian National University, Canberra.

Liao, J. C. (2004). Neuromuscular control of trout swimming in a vortex street: implications for energy economy during the Karman gait. *J. Exp. Biol.* **207**, 3495-3506.

Liao, J. C. (2007). A review of fish swimming mechanics and behaviour in altered flows. *Philos. Trans. R. Soc. B* **362**, 1973-1993.

Liao, J. C., Beal, D. N., Lauder, G. V. and Triantafyllou, M. S. (2003a). Fish exploiting vortices decrease muscle activity. *Science* **302**, 1566-1569.

Liao, J. C., Beal, D. N., Lauder, G. V. and Triantafyllou, M. S. (2003b). The Kármán gait: novel body kinematics of rainbow trout swimming in a vortex street. *J. Exp. Biol.* **206**, 1059-1073.

Lupandin, A. I. (2005). [Effect of flow turbulence on swimming speed of fish]. *Izv. Akad. Nauk. Ser. Biol.* **32**, 558-565.

Meijering, E., Dzyubachyk, O. and Smal, I. (2012). Methods for cell and particle tracking. *Methods Enzymol.* **504**, 183-200.

Methling, C., Tudorache, C., Skov, P. V. and Steffensen, J. F. (2011). Pop up satellite tags impair swimming performance and energetics of the European eel (*Anguilla anguilla*). *PLoS ONE* **6**, e20797.

Minetti, A. E., Ardigò, L. P., Capodaglio, E. M. and Saibene, F. (2001). Energetics and mechanics of human walking at oscillating speeds. *Am. Zool.* **41**, 205-210.

Mussi, M., Summers, A. P. and Domenici, P. (2002). Gait transition speed, pectoral fin-beat frequency and amplitude in *Cymatogaster aggregata*, *Embiotoca lateralis* and *Damalichthys vacca*. *J. Fish Biol.* **61**, 1282-1293.

Nakagawa, S., Schielzeth, H. and O'Hara, R. B. (2013). A general and simple method for obtaining R^2 from generalized linear mixed-effects models. *Methods Ecol. Evol.* **4**, 133-142.

Niimi, A. J. and Beamish, F. W. (1974). Bioenergetics and growth of largemouth bass (*Micropterus salmoides*) in relation to body weight and temperature. *Can. J. Zool.* **52**, 447-456.

Ohlberger, J., Staaks, G. and Hölker, F. (2007). Estimating the active metabolic rate (AMR) in fish based on tail beat frequency (TBF) and body mass. *J. Exp. Zool. A* **307**, 296-300.

Pavlov, D. S., Lupandin, A. I. and Skorobogatov, M. A. (2000). The effects of flow turbulence on the behaviour and distribution of fish. *J. Ichthyol.* **40**, S232-S261.

Peek, M. S., Russek-Cohen, E., Wait, D. A. and Forseth, I. N. (2002). Physiological response curve analysis using nonlinear mixed models. *Oecologia* **132**, 175-180.

Plaut, I. (2001). Critical swimming speed: its ecological relevance. *Comp. Biochem. Physiol.* **131A**, 41-50.

R Development Core Team (2010). R: a language and environment for statistical computing. Vienna. Austria: R Foundation for Statistical Computing. Available at: http://www.R-project.org.

Roche, D. G., Binning, S. A., Bosiger, Y., Johansen, J. L. and Rummer, J. L. (2013). Finding the best estimates of metabolic rates in a coral reef fish. *J. Exp. Biol.* **216**, 2103-2110.

Ruel, J. J. and Ayres, M. P. (1999). Jensen's inequality predicts effects of environmental variation. *Trends Ecol. Evol.* **14**, 361-366.

Steffensen, J. F., Johansen, K. and Bushnell, P. G. (1984). An automated swimming respirometer. *Comp. Biochem. Physiol.* **79A**, 437-440.

Steinhausen, M., Steffensen, J. F. and Andersen, N. (2005). Tail beat frequency as a predictor of swimming speed and oxygen consumption of saithe (*Pollachius virens*) and whiting (*Merlangius merlangus*) during forced swimming. *Mar. Biol.* **148**, 197-204.

Svendsen, J. C., Tudorache, C., Jordan, A. D., Steffensen, J. F., Aarestrup, K. and Domenici, P. (2010). Partition of aerobic and anaerobic swimming costs related to gait transitions in a labriform swimmer. *J. Exp. Biol.* **213**, 2177-2183.

Taguchi, M. and Liao, J. C. (2011). Rainbow trout consume less oxygen in turbulence: the energetics of swimming behaviors at different speeds. *J. Exp. Biol.* **214**, 1428-1436.

Tritico, H. M. and Cotel, A. J. (2010). The effects of turbulent eddies on the stability and critical swimming speed of creek chub (*Semotilus atromaculatus*). *J. Exp. Biol.* **213**, 2284-2293.

Tudorache, C., Jordan, A., Svendsen, J., Domenici, P., DeBoeck, G. and Steffensen, J. F. (2009). Pectoral fin beat frequency predicts oxygen consumption during spontaneous activity in a labriform swimming fish (*Embiotoca lateralis*). *Environ. Biol. Fishes* **84**, 121-127.

van de Pol, M. and Wright, J. (2009). A simple method for distinguishing within-versus between-subject effects using mixed models. *Anim. Behav.* **77**, 753-758.

Videler, J. J. (1993). *Fish Swimming*. London: Chapman & Hall.

Wardle, C. S., Soofiani, N. M., O'Neill, F. G., Glass, C. W. and Johnstone, A. D. F. (1996). Measurements of aerobic metabolism of a school of horse mackerel at different swimming speeds. *J. Fish Biol.* **49**, 854-862.

Webb, P. W. (1975). Hydrodynamics and energetics of fish propulsion. *Bull. Fish. Res. Bd Can.* **190**, 1-156.

Webb, P. W. (2006). Stability and maneuverability. In *Fish Biomechanics* (ed. R. E. Shadwick and G. V. Lauder), pp. 281-332. San Diego, CA: Academic Press.

Webb, P. W. and Cotel, A. J. (2010). Turbulence: does vorticity affect the structure and shape of body and fin propulsors? *Integr. Comp. Biol.* **50**, 1155-1166.

Webb, P. W., Cotel, A. and Meadows, L. A. (2010). Waves and eddies: effects on fish behavior and habitat distribution. In *Fish Locomotion: An Eco-Ethological Perspective* (ed. P. Domenici and B. G. Kapoor), pp. 1-39. Enfield, NH: Science Publishers.

Westneat, M. W. (1996). Functional morphology of aquatic flight in fishes: kinematics, electromyography, and mechanical modeling of labriform locomotion. *Am. Zool.* **36**, 582-598.

Wu, T. Y. (1977). Introduction to the scaling of aquatic animal locomotion. In *Scale Effects in Animal Locomotion* (ed. T. J. Pedley), pp. 203-232. New York, NY: Academic Press.

Fig. S1 Steffensen-type swimming respirometer for intermittent-flow respirometry. Panel A shows the different components of the respirometer, including the baffles, flow straightener and honeycomb used to produce near-laminar flow. Panel B shows the assembled respirometer with an external motor powering the propeller. Arrows indicate flow direction.
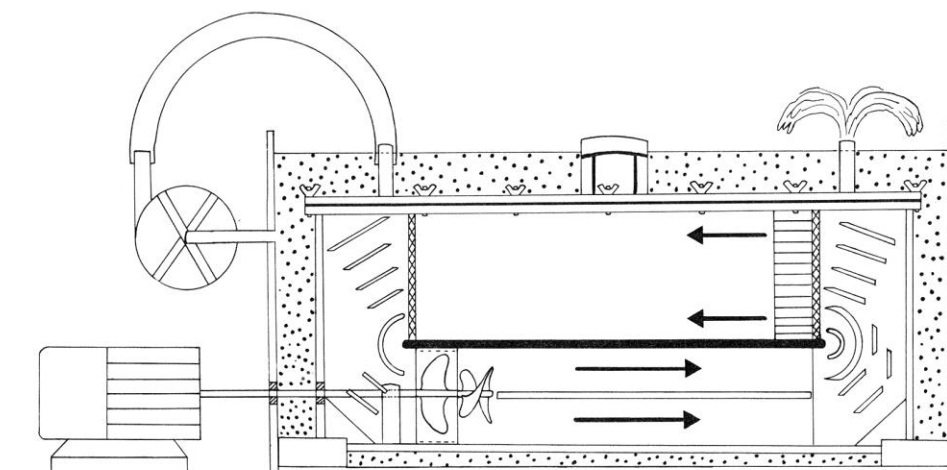
A)
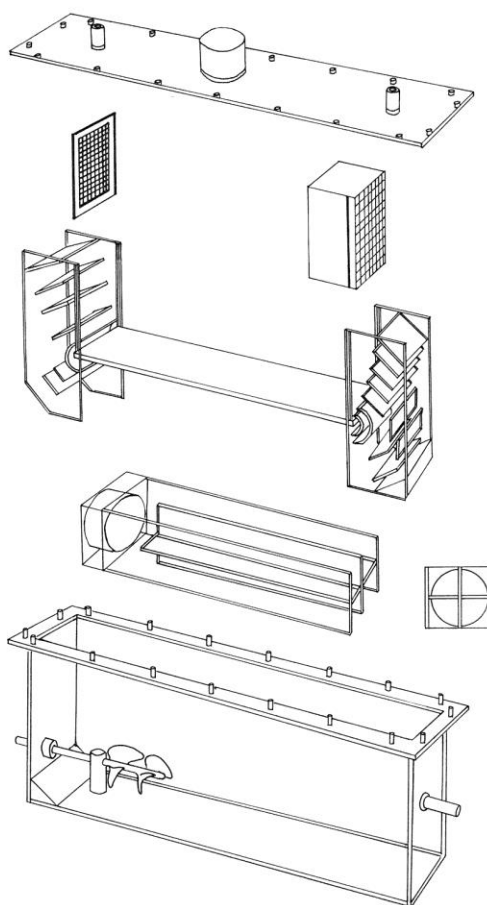
B)

Fig. S2 Example of flow characteristics in steady flow versus high unsteady flow for an average size fish (14.8 cm total length). Water flow velocity (cm s^{-1}) was obtained by tracking passive particles (neutrally buoyant expandable polystyrene beads with diameter < 1 mm, Foamex Polystyrene, Revesby, Australia) in the test section of the swim chamber at 0.033 Hz. Particles were tracked using the manual object tracking plugin MtrackJ for ImageJ (Meijering et al., 2012). Particles were tracked for 20 s in high unsteady flow (mean speed = 29.6 cm s^{-1} or 2 BLs^{-1}; amplitude = 1 BLs^{-1}; period = 5 s): the thick blue line indicates flow velocity in the x axis and the thick red line indicates absolute flow velocity in the y axis. The dashed grey line indicates the intended flow velocity. For comparative purposes, particles were tracked for 10 s in steady flow (mean speed = 29.6 cm s^{-1} or 2 BLs^{-1}): the thin blue line indicates flow velocity in the x axis and the thin orange line indicates absolute flow velocity in the y axis. Measures were obtained by averaging values obtained three times on the same video for both steady and unsteady flow; we averaged absolute values of velocity in y. Noise is partly due to small scale variation in flow speed and partly due to magnification of errors from the digitizing process (Walker, 1998). Descriptive statistics are presented in Table S1. Data are deposited in the figshare repository (DOI: 10.6084/m9.figshare.789064).
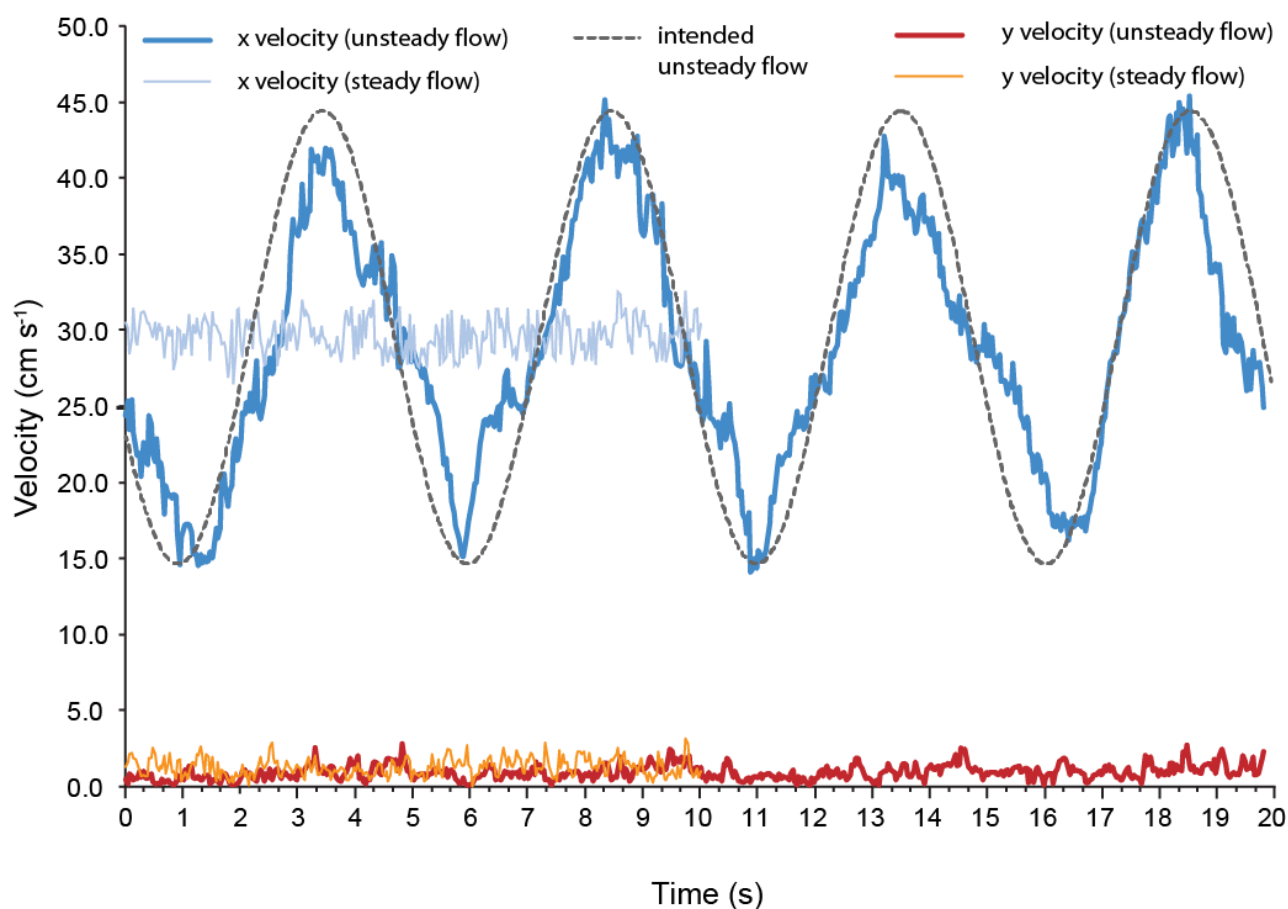
Meijering, E., Dzyubachyk, O. and Smal, I. (2012). Methods for cell and particle tracking. *Methods Enzymol.* **504**, 183-200.

Walker, J. A. (1998). Estimating velocities and accelerations of animal locomotion: A simulation experiment comparing numerical differentiation algorithms. *J. Exp. Biol.* **201**, 981-995.

Fig. S3 Same as Fig. S2, but showing (in green) the change in absolute vector angle of tracked passive particles at 0.033 Hz relative to the expected flow direction (i.e. measured vector vs. horizontal vector angle; Mv-Hv angle). Particles were tracked using the manual object tracking plugin MtrackJ for ImageJ (Meijering et al., 2012). Measures were obtained by averaging absolute values obtained three times on the same video for both steady and unsteady flow. The thick green line indicates the absolute Mv-Hv angle for particles tracked over 20 s in high unsteady flow (mean speed = 29.6 cm s^{-1} or 2 BLs^{-1}; amplitude = 1 Bl s^{-1}; period = 5 s). The thin green line indicates the absolute Mv-Hv angle for particles tracked over 10 s in steady flow (mean speed = 29.6 cm s^{-1} or 2 BLs^{-1}). The mean change in absolute Mv-Hv angle was 1.98° (range 0.00° – 4.76°) for steady flow and 2.47° (range 0.18° - 7.67°) for high unsteady flow. Other than velocity fluctuations in the x axis, flow conditions were similar in the two treatments and approximated near-laminar flow. Descriptive statistics are presented in Table S1. Data are deposited in the figshare repository (DOI: 10.6084/m9.figshare.789064).
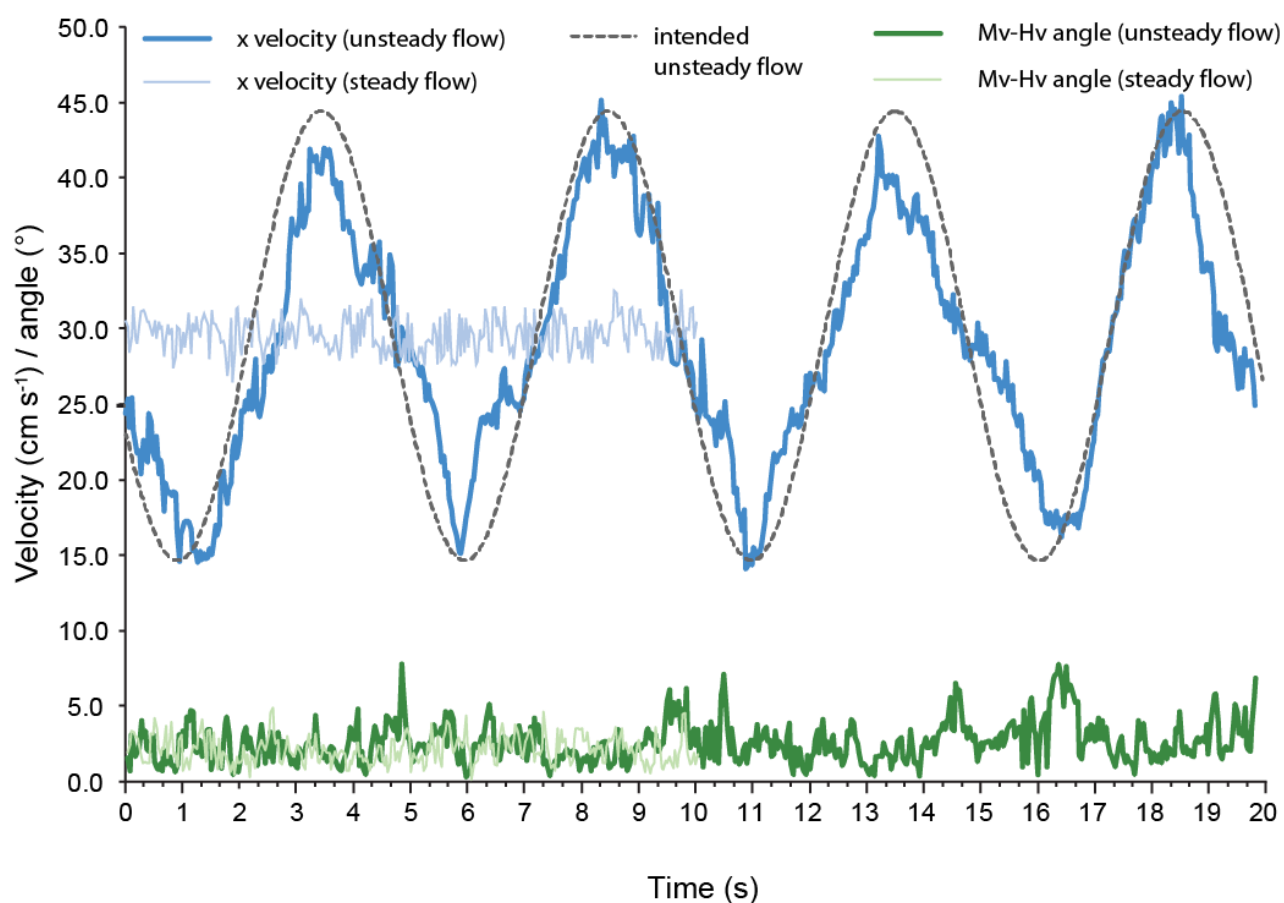
Movie 1. *Cymatogaster aggregata* swimming in high-amplitude unsteady flow. Fish exhibit high variation in fin beat period (T): T increases as flow velocity decreases, and decreases as flow velocity increases.

Table S1 Intended vs. observed flow characteristics (mean ± s.d.) for steady (mean speed = 29.6 cm s^{-1} or 2 BLs^{-1}) and high unsteady (mean speed = 29.6 cm s^{-1} or 2 BLs^{-1}; amplitude = 1 BLs^{-1}; period = 5 s) flow visualized in Figs S1 and S2.

Descriptor	Steady flow		High unsteady flow	
	Intended	*Observed*	*Intended*	*Observed*
Velocity in x (cm s^{-1})	29.60 ± 0.00	29.63 ± 1.18	29.60 ± 0.00	28.98 ± 7.98
Amplitude (cm s^{-1})	N/A	N/A	14.80 ± 0.00	15.03 ± 2.01
Velocity in y (cm s^{-1})	0.00 ± 0.00	-0.24 ± 0.84	0.00 ± 0.00	0.10 ± 0.70
Absolute velocity in y (cm s^{-1})	0.00 ± 0.00	1.27 ± 0.59	0.00 ± 0.00	0.93 ± 0.49
Mv-Hv angle (°)*	0.00 ± 0.00	-0.37 ± 1.37	0.00 ± 0.00	0.28 ± 2.04
Absolute Mv-Hv angle (°)*	0.00 ± 0.00	1.98 ± 0.92	0.00 ± 0.00	2.47 ± 1.36
Period (s)	N/A	N/A	5.00 ± 0.00	4.98 ± 0.28

* Vector angle relative to intended flow direction.